Manuscript submitted to: Volume 2, Issue 2, 116-130.

AIMS Biophysics DOI: 10.3934/biophy.2015.2.116

Received date 17 February 2015, Accepted date 05 May 2015, Published date 12 May 2015

Review

Recent Advances in Cryo-TEM Imaging of Soft Lipid Nanoparticles

Shen Helvig [1], Intan D. M. Azmi [1], Seyed M. Moghimi [2], and Anan Yaghmur [1,*]

[1] Department of Pharmacy, Faculty of Health and Medical Sciences, University of Copenhagen, Universitetsparken 2, 2100 Copenhagen Ø, Denmark

[2] Nanomedicine Laboratory, Center for Pharmaceutical Nanotechnology and Nanotoxicology, Department of Pharmacy, University of Copenhagen, DK-2100 Copenhagen Ø, Denmark

* **Correspondence:** E-mail: anan.yaghmur@sund.ku.dk; Tel: +45-3533-6541.

Abstract: Cryo-transmission electron microscopy **(**Cryo-TEM), and its technological variations thereof, have become a powerful tool for detailed morphological characterization and 3D tomography of soft lipid and polymeric nanoparticles as well as biological materials such as viruses and DNA without chemical fixation. Here, we review and discuss recent advances in Cryo-TEM analysis of lipid-based drug nanocarriers with particular emphasis on morphological and internal nanostructure characterization of lyotropic liquid crystalline nanoparticles such as cubosomes and hexosomes.

Keywords: cryo-TEM; cubosomes; 3D tomography; hexosomes; nanocarriers

1. Introduction

There is a growing interest in engineering *soft* self-assembled polymeric and lipid-based nanoparticles (e.g., polymer micelles, polymersomes, liposomes, niosomes, hexosomes, and cubosomes) for the solubilization, and efficient delivery of drugs and contrast agents to various sites in the body [1–12]. These approaches do not only modulate drug pharmacokinetics (e.g., volume of distribution and drug protection against premature degradation and removal, altered circulation half-lives) and biodistribution (e.g., improving safety through site-specific delivery and reducing the drug dose requirement), but further allow selection of those highly potent drugs that were discarded due to sever toxicity problems [2–6]. Furthermore, the surface of many of these carriers can be manipulated and functionalized with biological ligands such as folate, antibody molecules and their fragments, thus offering the possibilities for site-specific targeting to accessible sites in the body [7].

Many of the proposed drug nanocarriers still require design optimization for improving their biological performance (e.g., drug protection in biological fluids, cellular uptake and intracellular

trafficking processes), controlled/sustained drug release at the pathological sites, compartmental drug release, and in minimizing/overcoming infusion-related adverse reactions [13]. Indeed, characteristics such as size, shape and surface properties modulate biological performance of the engineered drug nanocarriers, and therefore it is important to develop analytical techniques that allow for precision biophysical characterization and of mapping 'structure-activity' parameters [1]. In this respect, an indispensable characterization technique is cryo-transmission electron microscopy (cryo-TEM), which allows direct morphological visualization of nanomaterials/nanoparticles as well as thin film sections of complex tissues at high spatial resolution, and at near native state [8–27]. Furthermore, with the latest technology advancement in data processing software and charged-coupled device (CCD) cameras, cryo-TEM can provide information on the 3-dimensional (3D) morphology of individual nanoparticles [15]. For instance, advancement in direct detectors has revolutionized cryo-TEM through very high quantum detector efficiency (QDE) that enables high signal-to-noise ratio (SNR). Here, we discuss the application of cryo-TEM for the morphological characteristics of *soft* self-assembled nanocarriers such as liposomes, cubosomes, and hexosomes.

1.1. Advantages and limitations

Cryo preparation is based on an ultra-fast conversion of a thin fluid suspension film into vitrified, low vapor pressure specimen for TEM [15]. This was first achieved by a plunging-freezing method, and it has also been adopted for imaging viruses, proteins, and nanomaterials [8,21]. The main advantage of using cryo-TEM is the preservation of the sample near its native state and the avoidance of any fixation of the sample. Indeed, sample fixation procedures may lead to lipid extraction, and may generate artifacts [28]. Since cryo-TEM can provide high-resolution images [9], it is the method of choice for studying samples where multiple structures with different morphology and size co-exist. More importantly, this method can capture metastable and short-lived intermediate species, and thus provide better understanding of self-assembly, phase transition mechanisms, and dynamic phenomena in complex lipid-based structures [9]. It should be emphasized that cryo-imaging is not a quantitative methodology and should be a part of an integrated analysis with quantitative biophysical techniques [23]. In this context, cryo-TEM is very useful when combined with small angle X-ray (SAXS) or neutron (SANS) scattering techniques, and self-diffusion NMR for detailed structural and morphological characterization of self-assembled nanostructures [22].

Despite numerous important advantages, a high level of expertise is still required for sample handling and data interpretation [14]. Care should be taken with sample handling, since many colloidal structures are sensitive to electron beam damage during imaging [15,23], or have low signal-to-noise ratio [15,23,24]. Careful sample preparation and handling is also required to avoid introduction of artifacts, such as ice crystals, which may affect image quality. Another important issue is the blotting procedure with filter paper during sample preparation, which may induce liquid flow and cause shear stress in the liquid leading either to a re-orientation of the dispersed objects or a morphological re-arrangement of the self-assembled structures [14].

2. Cryo-TEM Investigations of Soft Lipid Self-assembled Nanoparticles

Cryo-TEM is an essential tool for direct imaging of complex fluids. The versatility of cryo-TEM therefore permits morphological characterization of a wide range of particulate formulations. Recent

developments in the morphological and structural assessments of liquid crystalline nanoparticles, micellar solutions and microemulsions are described in this section.

2.1. Liposomes

Liposomes are vesicular structures consisting of an amphiphilic lipid or lipid mixtures forming bilayers enclosing hydrophilic domains in excess water. They are characterized by their membrane composition, morphology, and size [15]. Morphologically, the most common liposome types are small (S), large (L), unilamellar (U), oligolamellar (O), and multilamellar (ML) vesicles. Different characteristics of liposomes are controlled by their morphology and size, and these include encapsulation volume, deformability, thermotropic behavior, and aggregation state [8]. There is a growing interest in using cryo-TEM for investigating the effects of lipid composition and electrostatic interactions on the morphological features of these vesicles and for studying the influence of biological environment on their biophysical characteristics [27–31]. Also, cryo-TEM has widely been used for the structural and morphological assessment of liposome preparations as well as for detecting the structural changes that occur when encapsulating drugs or due to vesicular interaction with macromolecules such as polycations and nucleic acids [25–29]. For instance, drugs such as doxorubicin and mitoxantrone are efficiently encapsulated in liposomes through generation of a pH-gradient across the vesicular bilayer membrane [32]. This approach allows drug precipitation and crystallization in the vesicular aqueous space, where crystal growth can be visualized by cryo-TEM [15,25]. Indeed, the crystal morphology is important, since a long needle-shaped crystal may grow to an extent causing vesicular deformation or penetration through the bilayer causing vesicular rupture thus affecting vesicular stability and the overall formulation quality. Similarly, cryo-TEM studies have further revealed that some liposomal preparation, depending on their lipid composition, may contain stable planar and circular lipid disks that can be visualized in face-on and edge-on orientations [33].

2.2. Lyotropic liquid crystalline (LLC) nanoparticles

In addition to liposomes, dispersions of inverted type micellar solutions and lyotropic non-lamellar liquid crystalline phases are attractive systems for drug/contrast agent solubilization. Examples include cubosomes (aqueous dispersions with an internal inverted type 3D bicontinuous cubic (V_2) phase), hexosomes (aqueous dispersions with an internal inverted type 2D columnar hexagonal (H_2) nanostructure), micellar cubosomes (aqueous dispersions with an internal inverted type 3D discontinuous micellar cubic of the symmetry *Fd3m*), and emulsified microemulsion (EMEs), which are aqueous dispersions with an internal inverted type microemulsion (L_2 phase) [15,25,34]. Representative cryo-TEM images of these nanostructured aqueous dispersions are shown in Figure 1. Indeed, the highly ordered internal nanostructures of these lipid-based entities provide an extensive hydrophobic-hydrophilic interfacial area for the solubilization of different drugs, and notably hydrophobic molecules, thus offering a convenient way for drug administration into the body through different portals of entry [15,34].

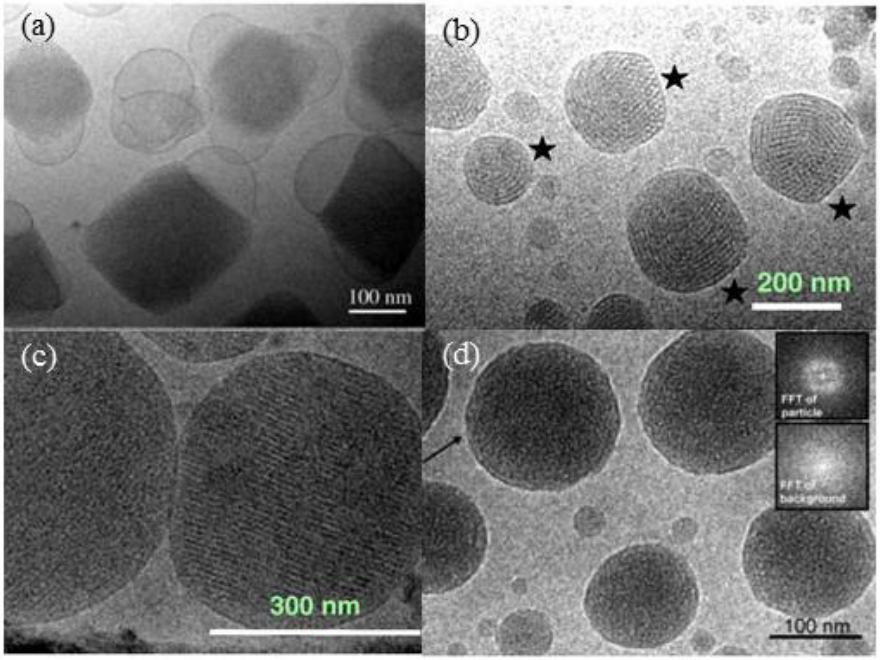

Figure 1. Cryo-TEM images of (a) cubosomes, (b) hexosomes, (c) micellar cubosomes, and (d) emulsified microemulsions (EMEs). In panel (d): the top inset is a FFT of the arrowed particle showing a diffuse peak of brightness and revealing the internal structure of the particle, and the bottom inset is a FFT of the background showing no peak of brightness in the surrounding aqueous medium. (Adapted with permission from Yaghmur et al. [43,44]).

Cryo-TEM has been used extensively in combination with SAXS or SANS to fully assess the morphology and the internal nanostructures of various types of non-lamellar liquid crystalline dispersions [37–56]. For instance, combination of cryo-TEM and SAXS was used to investigate the effect of increasing temperature and solubilizing a hydrophobic additive on the transition from cubosomes *via* hexosomes and micellar cubosomes to emulsified microemulsions (EMEs) [43,44,45]. Such integrative approaches are vital for development of lipidic non-lamellar liquid crystalline formulations with appropriate pharmaceutical attributes. For instance, combination of cryo-TEM with SAXS or SANS could be useful in the development of long-circulating injectable soft non-lamellar liquid crystalline nanocarriers by providing important information on the effect of PEGylation on the internal nanostructure, and the morphological characteristics of the nanoparticles (Figure 2) [46]. In a recent study [56], cryo-TEM revealed unique morphological features of lipidic nanoparticles consisting of three different nanostructures. Here, solubilization of carrier-free human recombinant brain-derived neurotrophic factor (BDNF) induced a transition from vesicles to cubosomes *via* an intermediate state consisting of different self-assembled nanostructures. These included an inner part consisting of coexisting lamellar and bicontinuous cubic diamond (*Pn3m*) phases, surrounded by a bicontinuous gyroid cubic (*Ia3d*) phase (Figure 3a, b). Cryo-TEM was also used as a complementary technique to SAXS for investigating a direct vesicles-to-cubosomes transition in monoelaidin (ME)-based aqueous dispersions [57]. In another study, SAXS and cryo-TEM were combined with cryo-field emission scanning electron microscopy (cyro-FESEM)

technique for investigating the internal nanostructures and 3D morphological features of cubosomes and hexosomes based on phytantriol. Cryo-FESEM was a useful tool for obtaining information on the 3D morphology of these non-lamellar liquid crystalline nanoparticles. The observed 3D "ball-like" morphology of cubosomes was consistent with the proposed mathematical models using a nodal surface representation. In case of hexosomes, the imaged particles showed "spinning-top" like structures [58].

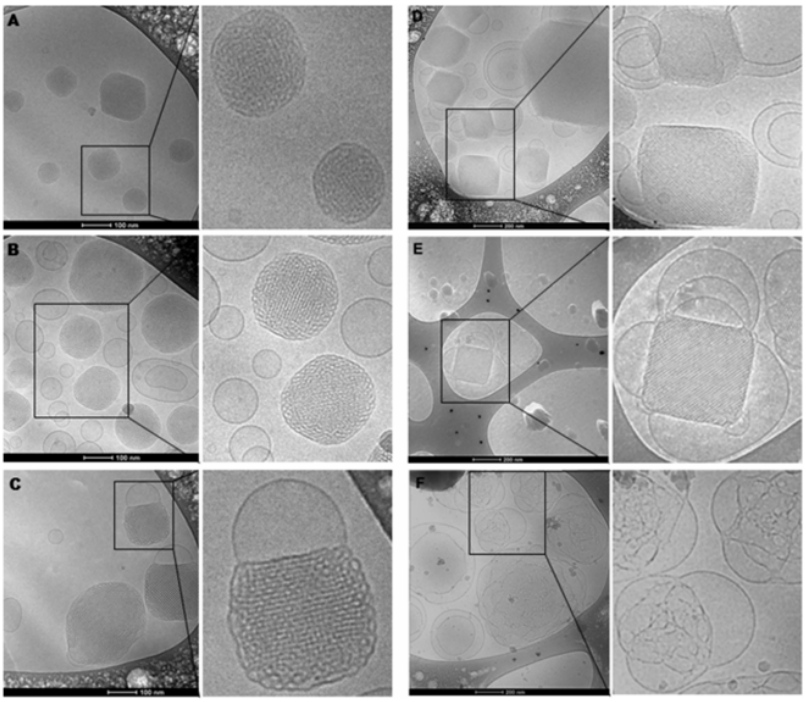

Figure 2. Cryo-TEM images of PEGylated cubosomes based on the binary mixture of phytantriol (PHYT)/DSPE-mPEG750 (A-C) and PHYT/DSPE-mPEG2000 (D-F). The binary lipid mixtures were prepared at the following weight ratios: 98:2 (panels A and D); 95:5 (panels B and E); and 90:10 (panels C and F), respectively. Scale bar: 100 nm (A-C) and 200 nm (D-F). (Adapted with permission from Nilsson et al. [46]).

It has also been possible to distinguish between different space groups of the internal cubic phases and to test the potential co-existence of more than one internal nanostructure in the dispersed liquid crystalline particles by controlling the tilting degree of the specimens in cryo-TEM [41,59]. This method particularly enables the discrimination between internal nanostructure of an inverted discontinuous micellar cubic (space group *Fd3m*), an inverted bicontinuous diamond (space group *Pn3m*) or an inverted bicontinuous primitive cubic structure (space group *Im3m*) (Figure 3c–f) [41,59]. In addition to classical cubosomes and hexosomes based on lipids with propensity to form non-lamellar phases, novel cubosomes formed from self-assembly of amphiphilic Janus dendrimers have been recently screened by cryo-TEM (Figure 4) [60].

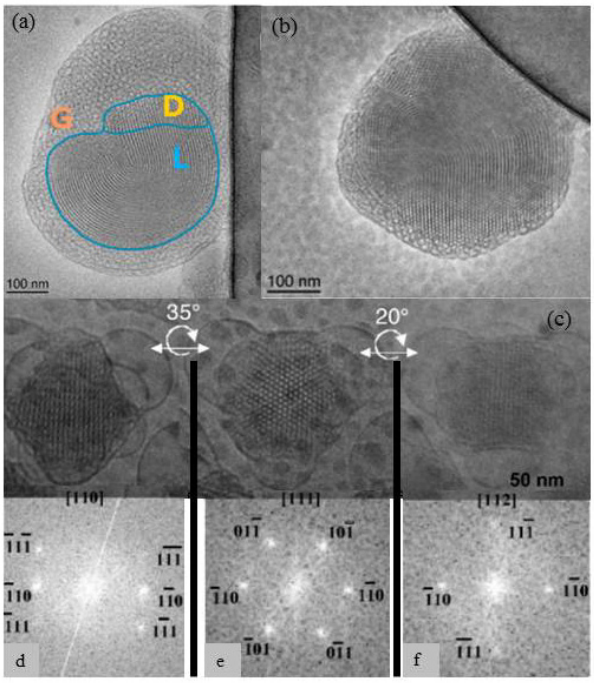

Figure 3. Cryo-TEM images of neurotrophin protein-loaded dispersion. (a) Three different phases detected; the blue line indicates the domain boundaries between the inner L, D, and G mesophases: L, lamellar; D, bicontinuous cubic *Pn3m* phase; and G, bicontinuous cubic *Ia3d* phase (b) an intermediate state that was detected during the transition from vesicles to cubosomes (adapted with permission from Angelov et al. [56]), (c) the tilt series of a particle having *Pn3m* cubic structure. The particle is viewed along [110]. (d) The corresponding intensity of the Fourier transform. (e) After 35º of tilting, the particle is viewed along [111], where a hexagonal motif is observed. (f) After 55º of tilting, the particle is now oriented along [112] (Adapted with permission from Sagalowicz et al. [59]).

There are many other studies that have used cryo-TEM for assessing the internal nanostructural arrangements of cubosomes and hexosomes of different lipid and surfactant compositions prior and after drug encapsulation [35–56] as well as their modulation by biological fluids such as plasma, lymph and tear. For instance, a recent integrated approach provided a comprehensive characterization of nanostructured aqueous dispersions on exposure to human plasma (Figure 5) [54]. Such investigations were conducted by combining cryo-TEM with SAXS and nanoparticle tracking analysis (NTA). Interestingly, it was shown that exposure to human plasma induced a modulatory effect on the size and morphological characteristics of the lipid nanoparticles, which was independent of dispersion-mediated complement activation processes and direct interactions with albumin. In principle, the applied experimental approach has considerable potential in future studies focusing on the design of safer and immune system compatible lyotropic liquid crystalline nanocarriers [54].

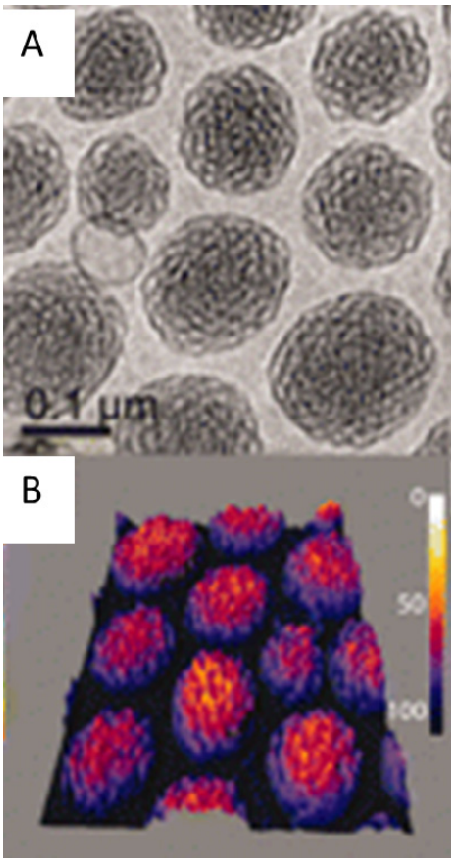

Figure 4. Self-assembly of amphiphilic Janus dendrimers. Cryo-TEM and 3D intensity profiles created using image J software (panels A and B) of cubosomes co-existing with low concentration of spherical dendrimersomes (Adapted with permission from Percec et al. [60]).

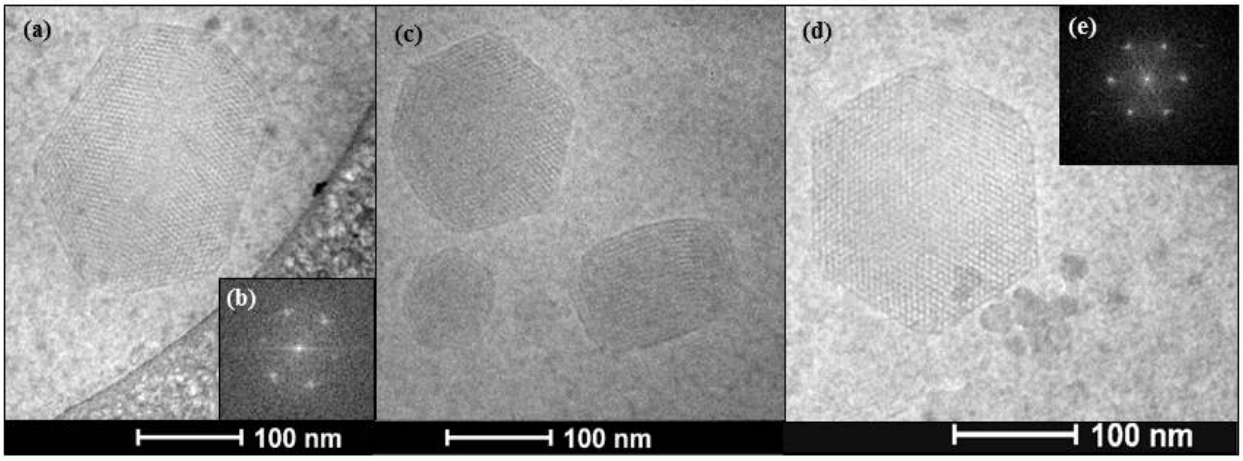

Figure 5. Cryo-TEM micrographs of PHYT dispersions and their Fast Fourier Transform (FFT) analysis. PHYT dispersions were mixed with human plasma at a ratio of 1:1 (v/v) and incubated for 17 h. Representative micrographs are shown in panels a, c and d. Panels b and e represent FFT analysis of the internal hexagonal (H_2) structure of hexosomes (Adapted with permission from Azmi et al. [54]).

Cryo-TEM images of lipid non-lamellar liquid crystalline dispersions can be subjected to fast Fourier transform (FFT) analysis, which allows assessment of the structural symmetry of the internal nanostructures, Figures 3, 5 and 6 [47–50]. Recently, FFT was employed to elucidate the internal nanostructure of radiolabeled cubosomes and hexosomes (Figure 6), confirming that radiolabelling had no deleterious effect on particle morphology and internal nanostructures [55]. In another study, FFT analysis was used to shed light on the effect of layer-by layer coating cubosomes with three different polymers (methacrylic acid-oleoyl methacrylate copolymer, poly (L-lysine), and poly (methacrylic acid)) on their morphological features and internal nanostructure [51].

In addition to cubosomes and hexosomes, time-resolved cryo-transmission electron microscopy (TRC-TEM) was used to investigate the dynamic structural events involved in the lamellar-to-inverted type hexagonal (L_α/H_2) phase transition in membrane dispersions [61]. This method provided deeper insight into the transition mechanism, which involved three distinct steps that were consistent with the "stalk" intermediates theory of membrane fusion [62].

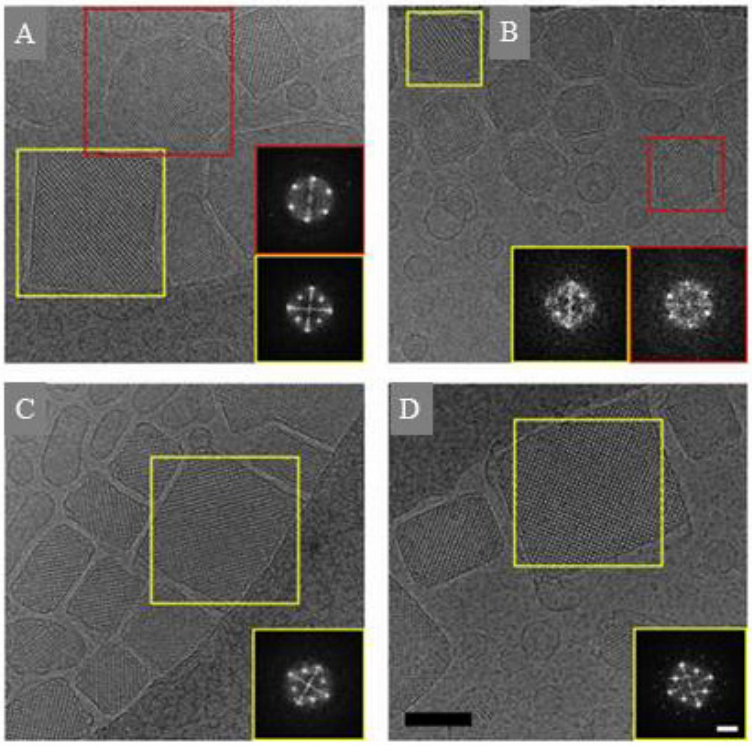

Figure 6. Cryo-TEM images of radiolabeled PHYT-based dispersions. (A) Binary PHYT/DSPE dispersion, at a weight ratio of 98/2; (B) ^{99m}Tc-HMPAO labeled binary PHYT/DSPE dispersion, at PHYT/DSPE weight ratio of 98/2; (C) binary PHYT/DSPE-PEG2000 dispersion with a weight ratio of 90/10; (D) ^{99m}Tc-HMPAO labeled binary PHYT/DSPE-PEG2000 dispersion with a PHYT/DSPE-PEG2000 weight ratio of 90/10. Red insets reveal the FFT analysis of the observed particles displaying internal inverted type hexagonal (H_2) nanostructure. Yellow insets display FFT analysis of dispersed particles of internal cubic symmetry. Scale bar: 100 nm. FFT scale bar: 5 nm. (Adapted with permission from Nilsson et al. [55]).

2.3. Micellar solutions and microemulsions

Micelles are dynamic self-assembled structures that are formed from surface-active molecules in an aqueous (normal-type micelles) or hydrophobic medium (inverted-type micelles), which can also be visualized by cryo-TEM, Figure 7. Both normal and reverse micellar solutions are capable of solubilizing a wide range of molecules [63–66]. In ternary or multi-component systems, the solubilization of either water in reverse micelles or oil in normal micelles leads to the formation of microemulsions, which are thermodynamically stable isotropic mixtures of oil, water and surfactant, frequently in combination with a co-surfactant or a co-solvent [66–69].

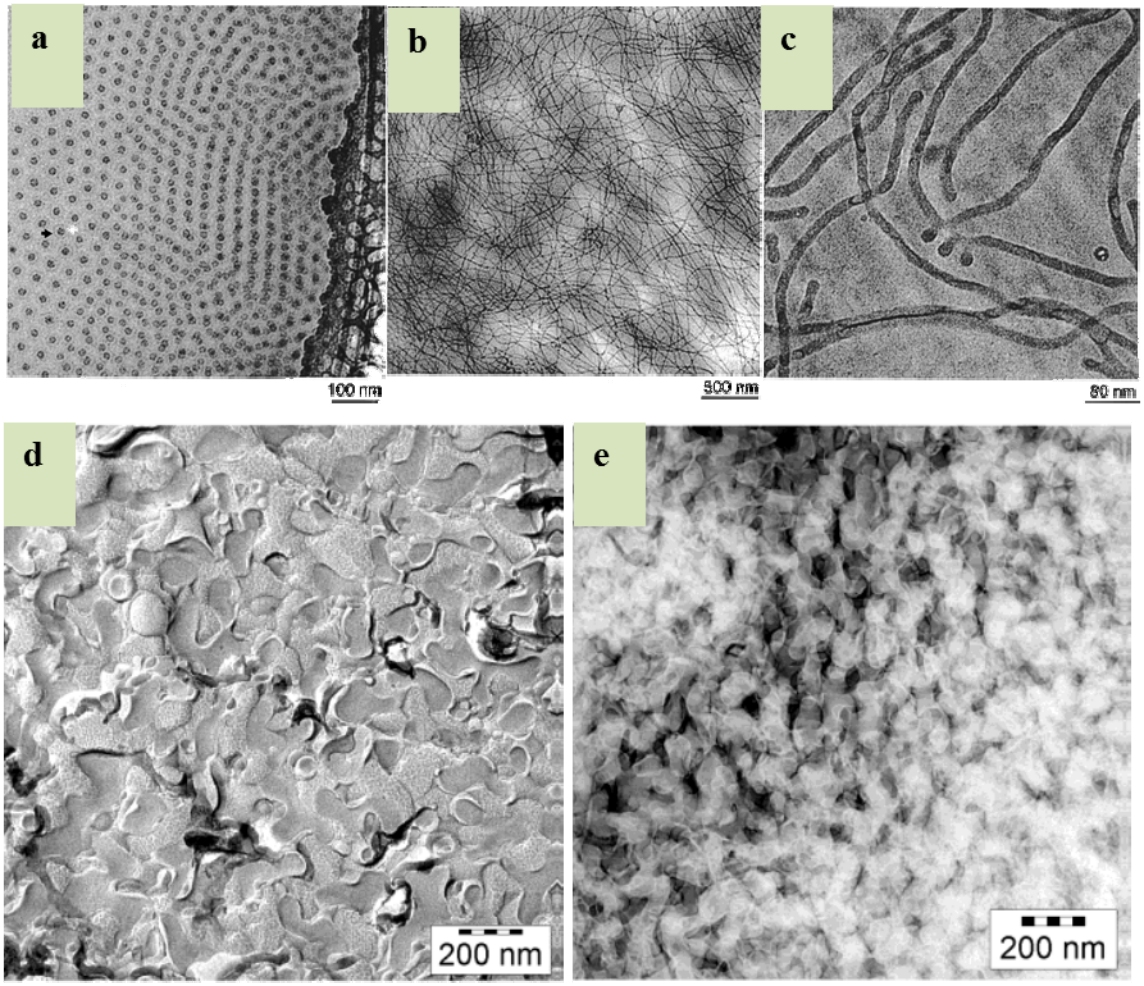

Figure 7. (a) Cryo-TEM images of spherical micelles from 1% block polymer (OB1) in water. Black arrow indicates the hydrated PEO, and white arrow shows the Fresnel fringe. 1% wormlike micelles at low (b) and higher (c) magnifications. Adapted from Won et al. [71] (d) Freeze Fracture EM micrograph of bicontinuous microemulsion based on the ternary H_2O-*n*-octane-$C_{12}E_5$ system compared to (e) Freeze Fracture Direct Image micrograph of the same sample. (Adapted from Belkoura et al. [70]).

Discrete microemulsions consist of domains of water (W/O) or oil (O/W) stabilized in a continuous hydrophobic or aqueous medium, whereas bicontinuous microemulsions consist of oil and water domains that are randomly distributed within the structure and separated by local interfaces. Microemulsions are becoming increasingly complex in their composition with the use of polymers, biomolecules and novel surfactants [69]. In recent years, cryo-TEM has made significant advances in this research topic by providing low radiation dose imaging possibilities of these otherwise delicate solutions [8]. In addition, less invasive and more reproducible cryogenic sample preparation method allows minimization of artifacts. This is an important aspect as microemulsions are often sensitive to the vigorous conditions of cryo-fixation that involves a high shear rate, risk of evaporating the specimen, and a possible molecular re-organization prior to freezing [64,69]. With an attempt of overcoming these challenges, Belkoura et al. [70] has proposed a novel approach by combining freeze-fracture with TEM. In this method, the sample is rapidly frozen, then fractured and viewed directly under TEM without the replication of the fracture. Indeed, this is a suitable approach for inverted type (W/O) and bicontinuous microemulsions (Figure 7 d, e), which are usually difficult to prepare and image by cryo-TEM [69]. This is also a non-blotting method, which can overcome issues related to applying a high shear rate that could affect the self-assembled structure [8,69,70].

2.4. Recent advances in 3D tomography

3D electron tomography is among the recent advances in this research field and it is considered as a sub-discipline of cryo-TEM, allowing for structural studies pertaining a single particle/entity [56]. In 3D tomography, a series of images are taken at a different tilt relative to the direction of the incident electron beam. These images could be combined using available computer programs to generate a 3D reconstruction of the sample specimen [72,73]. Limitations of this technique include the inability to image a complete angular range, i.e. angle coverage of $\pm 70^{o}$ instead of $\pm 90^{o}$. Another limitation is that the use of low radiation dose is necessary to minimize damage, however this yields low signal-to-noise ratio that could lead to poor quality of the images [74]. On the other hand, an averaging method could be employed during data analysis to obtain more detailed structural information than is present in the original tomogram [70]. Despite these limitations, this technique has been successfully used to analyze a wide range of biological structures in various contexts [72,75–84]. It also appears to hold real promises and to open new possibilities for the characterization of 3D morphology of nanoparticles in both material sciences and pharmaceutical fields. In particular, 3D electron tomography is expected to provide 3D characterization of polymeric and lipid-based nanocarriers with an improved resolution and to enlighten the self-assembly of surfactant-like lipids and polymers in 3D space. Such approaches may further provide more precise structural and morphological information on the influence of biological environment on the 3D morphology of lipid and polymer-based nanoparticles.

3. Conclusion

Cryo-TEM is a powerful tool with broad applicability to many biological specimens. It is also an emerging technology with enormous potential for performing high-resolution structural and morphological properties of soft lipidic and polymeric particles and investigating their behavior in biological environment. In the field of soft drug nanocarrier engineering, cryo-TEM is a frequently

used tool for the visualization of drug-free and drug-loaded liposomes, cubosomes and hexosomes and its use is expected to become more widespread in the pharmaceutical arena.

4. Future Challenges and Perspectives

With the steady progress of hardware and software development, better resolution, enhanced contrast, and reduced beam damage, cryo-TEM can further expand possibilities of imaging a wider range of drug delivery systems within an achievable time-frame. In particular, cryo-TEM with high resolution opens doors to advanced cryo-tomography that can provide valuable 3D information on the structure and morphology of biomolecules, drug-free and drug-loaded liposomes, cubosomes, hexosomes, and eventually might allow visualization of nanoparticle-cell interactions.

Acknowledgements

Financial support by the Danish Council for Independent Research | Technology and Production Sciences, reference 1335-00150b (to AY and SMM) is gratefully acknowledged. AY further acknowledges financial support from the Danish Natural Sciences Research Council (DanScatt).

Conflict of Interest

The authors declare no conflict of interests.

References

1. Moghimi SM, Hunter AC, Murray JC (2005) Nanomedicine: current status and future prospects. *FASEB J* 19: 311–330.
2. Grazú V, Moros M, Sánchez-Espinel C (2012) Nanobiotechnology - Inorganic Nanoparticles vs Organic Nanoparticles. *Front Nanosci* 4: 337–440.
3. Lim SB, Banerjee A, Önyüksel H (2012) Improvement of drug safety by the use of lipid-based nanocarriers. *J Control Release* 163: 34–45.
4. Nel AE, Maedler L, Velegol D, et al. (2009) Understanding biophysicochemical interactions at the nano-bio interface. *Nat Mater* 8: 543–557.
5. Couvreur P, Vauthier C (2006) Nanotechnology: intelligent design to treat complex disease. *Pharm Res* 23: 1417–1450.
6. Jin S-E, Jin H-E, Hong S-S (2014) Targeted delivery system of nanobiomaterials in anticancer therapy: from cells to clinics. *BioMed Res Int* 2014: 814208.
7. Moghimi SM, Peer D, Langer R (2011) Reshaping the future of nanopharmaceuticals: adiudicium. *ACS Nano* 5: 8454–8458.
8. Klang V, Valenta C, Matsko NB (2013) Electron microscopy of pharmaceutical systems. *Micron* 44: 45–74.
9. Danino D (2012) Cryo-TEM of soft molecular assemblies. *Curr Opin Colloid Interface Sci* 17: 316–329.
10. Danino D (2001) Digital cryogenic transmission electron microscopy: an advanced tool for direct imaging of complex fluids. *Colloids Surf A* 183-185: 113–122.

11. Burrows ND, Penn RL (2013) Cryogenic Transmission Electron Microscopy: Aqueous Suspensions of Nanoscale Objects. *Microsc Microanal* 19: 1542–1553.
12. Cho EJ, Holback H, Liu KC, et al. (2013) Nanoparticle characterization: State of the art, challenges, and emerging technologies. *Mol Pharm* 10: 2093–2110.
13. McNeil SE (2011) Challenges for nanoparticle characterization. *Methods Mol Biol* 697: 9–15.
14. Friedrich H, Frederik PM, de With G, et al. (2010) Imaging of self-assembled structures: interpretation of TEM and cryo-TEM images. *Angew Chem Int Ed Engl* 49: 7850–7858.
15. Kuntsche J, Horst JC, Bunjes H (2011) Cryogenic transmission electron microscopy (cryo-TEM) for studying the morphology of colloidal drug delivery systems. *Int J Pharm* 417: 120–137.
16. Rubino S, Akhtar S, Melin P, et al. (2012) A site-specific focused-ion-beam lift-out method for cryo Transmission Electron Microscopy. *J Struct Biol* 180: 572–576.
17. Frederik PM, Stuart MC, Bomans PH, et al. (1991) Perspective and limitations of cryo-electron microscopy. From model systems to biological specimens. *J Microsc* 161: 253–262.
18. Mielanczyk L, Matysiak N, Michalski M, et al. (2014) Closer to the native state. Critical evaluation of cryo-techniques for Transmission Electron Microscopy: preparation of biological samples. *Folia Histochem Cytobiol* 52: 1–17.
19. Pilhofer M, Ladinsky MS, McDowall AW, et al. (2010) Bacterial TEM: new insights from cryo-microscopy. *Methods Cell Biol* 96: 21–45.
20. De Carlo S, Harris JR (2011) Negative staining and cryo-negative staining of macromolecules and viruses for TEM. *Micron* 42: 117–131.
21. Adrian M, Dubochet J, Lepault J, et al. (1984) Cryo-electron microscopy of viruses. *Nature* 308: 32–36.
22. Fatouros DG, Müllertz A (2013) Development of Self-Emulsifying Drug Delivery Systems (SEDDS) for Oral Bioavailability Enhancement of Poorly Soluble Drugs. Drug Delivery Strategies for Poorly Water-Soluble Drugs: John Wiley & Sons Ltd. pp. 225–245.
23. Talmon Y (2007) Seeing giant micelles by cryogenic-temperature transmission electron microscopy (cryo-TEM). *Surfactant Sci Ser* 140: 163.
24. Spernath L, Regev O, Levi-Kalisman Y, et al. (2009) Phase transitions in O/W lauryl acrylate emulsions during phase inversion, studied by light microscopy and cryo-TEM. *Colloids Surf A* 332: 19–25.
25. Almgren M, Edwards K, Karlsson G (2000) Cryo transmission electron microscopy of liposomes and related structures. *Colloids Surf A* 174: 3–21.
26. Ferreira DA, Bentley MVLB, Karlsson G, et al. (2006) Cryo-TEM investigation of phase behaviour and aggregate structure in dilute dispersions of monoolein and oleic acid. *Int J Pharm* 310: 203–212.
27. Wytrwal M, Bednar J, Nowakowska M, et al. (2014) Interactions of serum with polyelectrolyte-stabilized liposomes: Cryo-TEM studies. *Colloids Surf B* 120: 152–159.
28. Fatouros DG, Bergenstahl B, Mullertz A (2007) Morphological observations on a lipid-based drug delivery system during in vitro digestion. *Eur J Pharm Sci* 31: 85–94.
29. Basáñez G, Ruiz-Argüello MB, Alonso A, et al. (1997) Morphological changes induced by phospholipase C and by sphingomyelinase on large unilamellar vesicles: a cryo-transmission electron microscopy study of liposome fusion. *Biophys J* 72: 2630–2637.
30. Phan S, Hawley A, Mulet X, et al. (2013) Structural aspects of digestion of medium chain triglycerides studied in real time using sSAXS and Cryo-TEM. *Pharm Res* 30: 3088–3100.

31. Alfredsson V (2005) Cryo-TEM studies of DNA and DNA–lipid structures. *Curr Opin Colloid Interface Sci* 10: 269–273.
32. Abraham SA, Edwards K, Karlsson G, et al. (2004) An evaluation of transmembrane ion gradient-mediated encapsulation of topotecan within liposomes. *J Control Release* 96: 449–461.
33. Johansson E, Lundquist A, Zuo S, et al. (2007) Nanosized bilayer disks: attractive model membranes for drug partition studies. *Biochim Biophys Acta* 1768: 1518–1525.
34. Yaghmur A, Glatter O (2009) Characterization and potential applications of nanostructured aqueous dispersions. *Adv Colloid Interface Sci* 147-148: 333–342.
35. Yaghmur A, Glatter O (2012) Self-Assembly in Lipidic Particles. Self-Assembled Supramolecular Architectures: Lyotropic Liquid Crystals: John Wiley & Sons pp. 129–155.
36. Yaghmur A, Rappolt M (2012) Structural characterization of lipidic systems under nonequilibrium conditions. *Eur Biophys J* 41: 831–840.
37. Nilsson C, Edwards K, Eriksson J, et al. (2012) Characterization of oil-free and oil-loaded liquid-crystalline particles stabilized by negatively charged stabilizer citrem. *Langmuir* 28: 11755–11766.
38. Hedegaard SF, Nilsson C, Laurinmaki P, et al. (2013) Nanostructured aqueous dispersions of citrem interacting with lipids and PEGylated lipids. *RSC Adv* 3: 24576–24585.
39. Chang DP, Jankunec M, Barauskas J, et al. (2012) Adsorption of lipid liquid crystalline nanoparticles: effects of particle composition, internal structure, and phase behavior. *Langmuir* 28: 10688–10696.
40. Siegel DP, Burns JL, Chestnut MH, et al. (1989) Intermediates in membrane fusion and bilayer/nonbilayer phase transitions imaged by time-resolved cryo-transmission electron microscopy. *Biophys J* 56: 161–169.
41. Barauskas J, Johnsson M, Tiberg F (2005) Self-assembled lipid superstructures: beyond vesicles and liposomes. *Nano Lett* 5: 1615–1619.
42. Janiak J, Bayati S, Galantini L, et al. (2012) Nanoparticles with a bicontinuous cubic internal structure formed by cationic and non-ionic surfactants and an anionic polyelectrolyte. *Langmuir* 28: 16536–16546.
43. Yaghmur A, De Campo L, Sagalowicz L, et al. (2005) Emulsified microemulsions and oil-containing liquid crystalline phases. *Langmuir* 21: 569–577.
44. Yaghmur A, de Campo L, Salentinig S, et al. (2006) Oil-loaded monolinolein-based particles with confined inverse discontinuous cubic structure (Fd3m). *Langmuir* 22: 517–521.
45. de Campo L, Yaghmur A, Sagalowicz L, et al. (2004) Reversible Phase Transitions in Emulsified Nanostructured Lipid Systems. *Langmuir* 20: 5254–5261.
46. Nilsson C, Østergaard J, Larsen SW, et al. (2014) PEGylation of phytantriol-based lyotropic liquid crystalline particles-the effect of lipid composition, PEG chain length, and temperature on the internal nanostructure. *Langmuir* 30: 6398–6407.
47. Sagalowicz L, Michel M, Adrian M, et al. (2006) Crystallography of dispersed liquid crystalline phases studied by cryo-transmission electron microscopy. *J Microsc* 221: 110–121.
48. Gao M, Kim Y-K, Zhang C, et al. (2014) Direct observation of liquid crystals using cryo-TEM: specimen preparation and low-dose imaging. *Microsc Res Tech* 77: 754–772.
49. Angelova A, Angelov B, Drechsler M, et al. (2013) Protein entrapment in PEGylated lipid nanoparticles. *Int J Pharm* 454: 625–632.
50. Sagalowicz L, Mezzenga R, Leser ME (2006) Investigating reversed liquid crystalline

mesophases. *Curr Opin Colloid Interface Sci* 11: 224–229.
51. Driever CD, Mulet X, Waddington LJ, et al. (2013) Layer-by-layer polymer coating on discrete particles of cubic lyotropic liquid crystalline dispersions (cubosomes). *Langmuir* 29: 12891–12900.
52. Oliveira IMSC, Silva JPN, Feitosa E, et al. (2012) Aggregation behavior of aqueous dioctadecyldimethylammonium bromide/monoolein mixtures: a multitechnique investigation on the influence of composition and temperature. *J Colloid Interface Sci* 374: 206–217.
53. Bode JC, Kuntsche J, Funari SS, et al. (2013) Interaction of dispersed cubic phases with blood components. *Int J Pharm* 448: 87–95.
54. Azmi IDM, Wu L, Wibroe PP, et al. (2015) Modulatory effect of human plasma on the internal nanostructure and size characteristics of liquid crystalline nanocarriers. *Langmuir* 31: 5042–5049.
55. Nilsson C, Barrios-Lopez B, Kallinen A, et al. (2013) SPECT/CT imaging of radiolabeled cubosomes and hexosomes for potential theranostic applications. *Biomaterials* 34: 8491–8503.
56. Angelov B, Angelova A, Filippov SK, et al. (2014) Multicompartment lipid cubic nanoparticles with high protein upload: millisecond dynamics of formation. *ACS Nano* 8: 5216–5226.
57. Yaghmur A, Laggner P, Almgren M, et al. (2008) Self-assembly in monoelaidin aqueous dispersions: direct vesicles to cubosomes transition. *PLoS ONE* 3: e3747.
58. Rizwan SB, Dong Y-D, Boyd BJ, et al. (2007) Characterisation of bicontinuous cubic liquid crystalline systems of phytantriol and water using cryo field emission scanning electron microscopy (cryo FESEM). *Micron* 38:478–485.
59. Sagalowicz L, Acquistapace S, Watzke HJ, et al. (2007) Study of liquid crystal space groups using controlled tilting with cryogenic transmission electron microscopy. *Langmuir* 23: 12003–12009.
60. Percec V, Wilson DA, Leowanawat P, et al. (2010) Self-assembly of Janus dendrimers into uniform dendrimersomes and other complex architectures. *Science* 328: 1009–1014.
61. Siegel DP, Epand RM (1997) The mechanism of lamellar-to-inverted hexagonal phase transitions in phosphatidylethanolamine: implications for membrane fusion mechanisms. *Biophys J* 73: 3089–3111.
62. Siegel DP, Green WJ, Talmon Y (1994) The mechanism of lamellar-to-inverted hexagonal phase transitions: a study using temperature-jump cryo-electron microscopy. *Biophys J* 66: 402–414.
63. Ansari MJ, Kohli K, Dixit N (2008) Microemulsions as potential drug delivery systems: a review. *PDA J Pharm Sci Technol* 62: 66–79.
64. Lawrence MJ, Rees GD (2000) Microemulsion-based media as novel drug delivery systems. *Adv Drug Delivery Rev* 45: 89–121.
65. Chatzidaki MD, Mitsou E, Yaghmur A, et al. (2015) Formulation and characterization of food-grade microemulsions as carriers of natural phenolic antioxidants. *Colloid Surf A* Doi: 10.1016/j.colsurfa.2015.03.060.
66. Yaghmur A., Aserin A, Garti N (2002) Phase behavior of microemulsions based on food-grade nonionic surfactants: effect of polyols and short-chain alcohols. *Colloids Surf A* 209:71–81.
67. Chevalier Y, Zemb T (1990) The Structure of Micelles and Microemulsions. *Rep Prog Phys* 53: 279–371.
68. Strey R (1994) Microemulsion microstructure and interfacial curvature. *Colloid Polym Sci* 272: 1005–1019.

69. Gradzielski M (2008) Recent developments in the characterisation of microemulsions. *Curr Opin Colloid Interface Sci* 13: 263–269.
70. Belkoura L, Stubenrauch C, Strey R (2004) Freeze fracture direct imaging: A new freeze fracture method for specimen preparation in cryo-transmission electron microscopy. *Langmuir* 20: 4391–4399.
71. Won YY, Brannan AK, Davis HT, et al. (2002) Cryogenic transmission electron microscopy (cryo-TEM) of micelles and vesicles formed in water by polyethylene oxide-based block copolymers. *J Phys Chem B* 106: 3354–3364.
72. Subramaniam S, Milne JL (2004) Three-dimensional electron microscopy at molecular resolution. *Annu Rev Biophys Biomol Struct* 33: 141–155.
73. Milne JLS, Borgnia MJ, Bartesaghi A, et al. (2013) Cryo-electron microscopy--a primer for the non-microscopist. *FEBS J* 280: 28–45.
74. Lengyel J, Milne JLS, Subramaniam S (2008) Electron tomography in nanoparticle imaging and analysis. *Nanomedicine* 3: 125–131.
75. Hoenger A, Bouchet-Marquis C (2011) Cellular tomography. *Adv Protein Chem Struct Biol* 82: 67–90.
76. Hurbain I, Sachse M (2011) The future is cold: cryo-preparation methods for transmission electron microscopy of cells. *Biol Cell* 103: 405–420.
77. Milne JL, Subramaniam S (2009) Cryo-electron tomography of bacteria: progress, challenges and future prospects. *Nat Rev Microbiol* 7: 666–675.
78. Tocheva EI, Li Z, Jensen GJ (2010) Electron cryotomography. *Cold Spring Harb Perspect Biol* 2: a003442.
79. Pierson J, Vos M, McIntosh JR, et al. (2011) Perspectives on electron cryo-tomography of vitreous cryo-sections. *J Electron Microsc (Tokyo)* 60 Suppl 1: S93–100.
80. Subramaniam S, Bartesaghi A, Liu J, et al. (2007) Electron tomography of viruses. *Curr Opin Struct Biol* 17: 596–602.
81. Yahav T, Maimon T, Grossman E, et al. (2011) Cryo-electron tomography: gaining insight into cellular processes by structural approaches. *Curr Opin Struct Biol* 21: 670–677.
82. Wisedchaisri G, Reichow SL, Gonen T (2011) Advances in structural and functional analysis of membrane proteins by electron crystallography. *Structure* 19: 1381–1393.
83. Orlova EV, Saibil HR (2011) Structural analysis of macromolecular assemblies by electron microscopy. *Chem Rev* 111: 7710–7748.
84. Frank J (2009) Single-particle reconstruction of biological macromolecules in electron microscopy—30 years. *Q Rev Biophys* 42: 139–158.